Indian Journal of Pure & Applied Physics
Vol. 61, June 2023, pp. 389-400
DOI: 10.56042/ijpap.v61i6.2405

An Investigation of Radiological Risk in Test Dwelling through Experimental and Simulation Approaches

Vandana Devi[a*], Era Garg[b] & R P Chauhan[a]

[a]Department of Physics, National Institute of Technology, Kurukshetra, Haryana 136 119, India

[b]Department of Chemistry, IB PG College Panipat, Haryana 132 103, India

Received 20 February 2023; accepted 23 May 2023

Study of radon, thoron and their progeny are important from radiological point of view. This work is towards their prediction, measurement, decay behavior, estimation of associated factors and effective dose for different room conditions (open and closed). The levels are measured experimentally using active monitors, dosimeters and deposition-based progeny sensors. Radon is found uniformly distributed for the open room condition while thoron shows complex behavior. A decrease in radon concentration is found through prediction and measurement for open room condition with increase of homogeneity. The solid radon progenies got distributed uniformly in the closed room. Total equilibrium equivalent concentration (EEC) for thoron is found comparatively more for the open room condition, EEC (unattached) found more for the closed environment, while for radon both are higher for closed room condition. The gas levels along with distribution are found to be affected by the vent ambiance. The average of unattached factors is estimated to be f_{Rn} (0.1) for open, (0.2) for closed while f_T (0.1) for open, (0.3) for closed room. Comparison of measurement and simulation approach shows reasonable matching of the results and validation of the simulation code. Different doses and conversion factors are also estimated and found within the recommended limits.

Keywords: Indoor radon; Dosimeter; Active radon measurement; DRPS; DTPS

1 Introduction

The impetus of exploring radon, thoron and their decay products is because of their significant contribution to total dose (about 55%)[1-2]. Being a gas, radon diffuses from the generation site to the environment. In the outdoor environment, it dilutes with the atmospheric air resulting in lesser concentration levels. Indoor radon (^{222}Rn) can either radiate from the underneath soil or used construction material, that can mount up to different levels depending upon dwellings ventilation conditions[3-4]. Residents exposed to radioactive gas are having radiological doses and hence health risks. Thoron (^{220}Rn) because of comparatively shorter half-life ignored earlier but studies show for some conditions its level may be large and that can lead to higher inhalation dose also. Progenies of ^{222}Rn and ^{220}Rn, couple to circumjacent particles and enter the respiratory system and irradiate. These radiations out turn tissue damage, which can ultimately lead to health-related risks[5-8].

Radon and thoron have been studied by researchers using different experimental techniques for different dwellings. Dispersion studies presented, are mostly based on the simulation results[9-10]. Study related to ^{220}Rn and its progeny has been a part of only a few exposure surveys in literature[11-13]. Accordingly, health related risk analysis, rather to rely on average concentrations only should also be checked by taking different conditions into account, hence the behavior and dispersion are vital to investigate. A combined and comparative radon-thoron study along with the progeny is carried out for a common Indian room environment taking different ventilation into account by opening and closing the ventilation openings present in the room. The paper includes the combined study of active-passive measurements and CFD simulation. Associated factors such as equilibrium factor, unattached fraction, dose conversion factors (DCFs), inhalation dose, effective dose, etc. are also estimated. A discussion is made on comparing the results for different room conditions and measurement methods along with the comparative behavior of ^{222}Rn and ^{220}Rn. The objective is to understand the ^{222}Rn, ^{220}Rn and decay products for different ventilation conditions and their variation with different measuring positions. Such monitoring studies targeted the exposure dose as the quantities of radiation protection considerations.

*Corresponding author: (E-mail: vandanac821@gmail.com)

2 Methods and Measurements

2.1 Study Room Description

An experimental room with volume of 28.44 m^3 (length: 3.16 m; width: 3 m; height: 3 m) is selected. Dwellings in India are primarily made up of soil, sand, bricks, cemented bricks and marble. Various granite types are sometimes also used for walls, flooring and kitchens. The study room geometry is shown in Fig. 1. The room is made up of bricks and plaster, soil is present underneath the floor which itself is furnished with sand, cement and concrete mixture. Building construction materials contribute to radioactive gas radon and thoron through six-room surfaces. One door is present in the room with area (1.6 m^2) on the front wall while the window with area (2 m^2) is present on the opposite wall. The experimental study is carried out by dividing the room in three equidistant planes P1, P2 and P3 at 0.8m, 1.6m and 2.4 m height from floor respectively. (Fig. 1)

2.2 Experimental Techniques

Indoor ^{222}Rn and ^{220}Rn are measured with twin cup dosimeters having pin-hole arrangement and scintillation radon-thoron monitor (SRM-STM) at desired locations. Attached and unattached equilibrium equivalent ^{222}Rn/^{220}Rn concentration (EERC/EETC) are evaluated using direct and wire-mesh-capped deposition-based progeny sensors for ^{222}Rn/^{220}Rn (DRPS/DTPS) by suspending inside. Calibration of the devices is carried out at the Radiological Physics and Advisory Division, BARC, Mumbai, India. Source flux measurements are carried out using SRM/STM and accumulator.

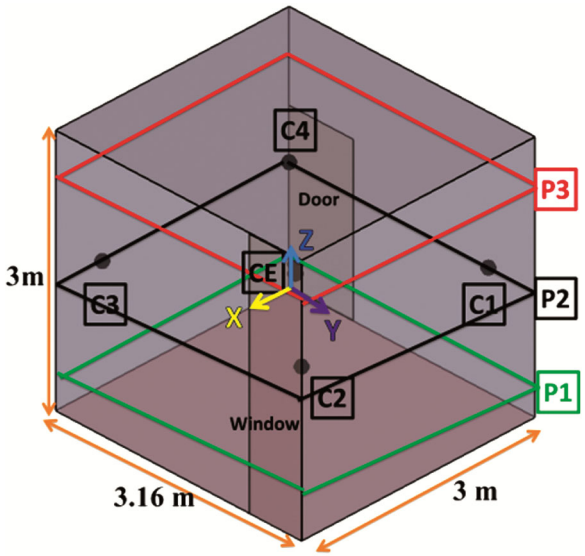

Fig. 1 — Experimental room geometry model.

2.2.1 Active monitoring of radon-thoron and flux measurement

^{222}Rn and ^{220}Rn concentration sare measured actively using radon (SRM) and thoron (STM) monitors based on scintillation. The active measurement devices are based on scintillation produced and the total number of counts converted into concentration using an inbuilt algorithm. Measurements are carried out with diffusion mode for SRM and flow mode for STM details are given elsewhere[14-15]. In diffusion mode, ^{220}Rncannot enter the scintillation cell due to the pin-hole plate while ^{222}Rn measurement. The radon and thoron concentrations are displayed in Bqm^{-3} on the monitor display.

As a necessary input for simulation, the flux from the room surfaces is estimated using the scintillation monitor and the gas accumulator arrangement[15-16]. For the measurement of flux, the gas accumulation chamber is fixed on the surface whose flux is to be measured and allowed the gas to accumulate after exhalation from the surface. The chamber should be fixed tightly to assure no leakage. A pump with power controlled by a scintillation monitor is used and the connected monitor displays the concentration in Bqm^3. The flux observed with the linear fitting of concentration and time data[15-16].

2.2.2 Passive Measurement of ^{222}Rn and ^{220}Rn

Single-entry pinhole-based twin cup dosimeters are used for time-integrated radon and thoron gas concentrations evaluation at desired locations. It consists of two partitions having pin-hole circular disk (to suppress thoron entry) as separation discussed elsewhere[17]. Gas rip off the filter paper (gas fiber-0.56 μm)to enter the first chamber (^{222}Rn + ^{220}Rn chamber) and then enters the second (^{222}Rn chamber) after passing pin holes arrangement. The radon (C_R) and thoron (C_T) concentrations are evaluated using Eq. (1) and (2) respectively.

$$C_R = \frac{T_1}{t\ x\ K_R} \tag{1}$$

$$C_T = \frac{T_2 - tC_R K_R'}{t\ x\ K_T} \tag{2}$$

Where t (days) refers to the total time during exposure, Track densities ($T_1$and T_2)(tracks/cm^2) observed in^{222}Rn and (^{222}Rn +^{220}Rn)chamber, respectively and the calibration factor of radon in ^{222}Rn chamber is K_R(0.0170 ± 0.002 tracks/cm^2/d/Bq/m^3). K'_R (0.0172 ± 0.002) and K_T (0.010 ± 0.001) are the calibration factor (tracks/cm^2/d/Bq/m^3) of radon and thoron respectively in (^{222}Rn + ^{220}Rn) chamber[17].

2.2.3 Equilibrium equivalent concentrations measurement: EERC and EETC

Equilibrium equivalent ^{222}Rn/^{220}Rn concentrations (EERC/EETC) are measured using deposition-based progeny sensors named direct radon/thoron progeny sensor (DRPS/DTPS)[18-19]. The sensors DRPS and DTPS have an arrangement of the detector (LR-115) covered with different thicknesses of absorber for ^{222}Rn and ^{220}Rn for EEC estimation. In the DRPS an absorber of 37 μm effective thickness was used to identify α- particles having 7.69 MeV energy and that of 50 μm was taken for 8.78 MeV α-particles in DTPS. Thoron progeny (^{212}Po) also registers tracks in DRPS because of its high energy compared to radon progeny (^{214}Po) and the less thickness of absorber used. The tracks due to radon progeny only (T_{Rn}) in DRPS are evaluated by eliminating tracks in DTPS (T_{DTPS}) from that in DRPS (T_{DRPS}) (Eq. 3)[18]. EERC and EETC are calculated using the relation (4) and (5)[20].

$$T_{Rn} = T_{DRPS-} \frac{\eta_{RT}}{\eta_{TT}} T_{DTPS} \quad (3)$$

$$\text{EERC} = \frac{\text{T}_{\text{Rn}} - \text{B}}{\text{t x S}_{\text{R}}} \quad (4)$$

$$\text{EETC} = \frac{\text{T}_{\text{T}} - \text{B}}{\text{t x S}_{T}} \quad (5)$$

η_{RT}(0.01 ± 0.0004) is the track registration efficiency for ^{220}Rn progeny in DRPS and η_{TT}(0.083 ± 0.004) for ^{220}Rn progeny in DTPS. S_R(0.09 ± 0.0036) and S_T (0.94 ± 0.027) refers to the sensitivity factor in tracks/cm^2/d/EERC(Bq/m^3) for^{222}Rn and ^{220}Rn progeny. And T_T is the track density in DTPS[18-19].

2.2.4 Measurement of unattached and attached EERC/EETC concentrations

The attached progeny fractions are measured by differently designed DRPS and DTPS covered with a wire mesh screen on which the coarse fractions get deposited. And the tracks are produced due to the associated activity with deposited fraction. Progeny concentration in attached form can be estimated using relations (4) and (5). Here S_R used is 0.034 and S_T is 0.33 used[19]. The simple DRPS/DTPS gives the total EEC (EEC_{U+A}) while the unattached EEC (EEC_U) is calculated by eliminating the attached EEC (EEC_A) from the total EEC. The unattached radon (f_{Rn}) and thoron fraction (f_T) is defined as the fraction of the potential alpha energy concentration (PAEC) of short-lived progeny present in an unattached form in the surrounding. f_{Rn} and f_T are evaluated as the ratio of unattached EEC to total EEC using following relation[21-22].

$$f = \frac{\text{EEC}_{\text{U}}}{\text{EEC}_{\text{U+A}}} \quad (6)$$

Also, the ^{222}Rn and ^{220}Rn equilibrium factors F_{Rn} and F_T respectively were evaluated as the ratio of $\text{EEC}_{\text{A+U}}$ to radon and thoron concentration respectively by using Eq.(7)[22-23].

$$F = \frac{\text{EEC}_{\text{U+A}}}{\text{C}_{\text{Rn or T}}} \quad (7)$$

The pelliculable LR- 115 detectors were fixed in the detectors on the holders provided and are retrieved after exposure to etched without stirring in NaOH solutions (2.5 N) for 1.5 hours at 60 °C in the etching bath. The tracks counting was done with a spark counter on the peeled-off detector from the cellulose nitrate base at optimized operating and pre-sparking voltage.

2.2.5 Dose calculations

The annual effective dose for ^{222}Rn and ^{220}Rn(*AEDR* and *AEDT*)received by residents in the indoor environment from ^{222}Rn, ^{220}Rn and their progeny concentrations are calculated using the following relation stated[1,24].

$$AEDR\ (mSv/y) = [(C_R x\ 0.17) + (EERC\ x\ 9)]\ x\ 8760\ h\ x\ 0.8\ x\ 10^{-6} \quad (8)$$

$$AEDT\ (mSv/y) = [(C_T x\ 0.11) + (EETC\ x\ 40)]\ x\ 8760\ h\ x\ 0.8\ x\ 10^{-6} \quad (9)$$

Where, the dose conversion factor (DCFs) in nSv $Bq^{-1}h^{-1}m^3$ are 0.17 and 9 for radon gas and EERC respectively whereas those for C_T and EETC are 0.11 and 40 respectively.

The effective dose from radon decay product exposure is estimated using the dose conversion factors that relate exposure to inhalation dose. Individually DCFs for mouth and nasal can be estimated. The DCFs estimation for mouth (DCF_M) and nasal (DCF_N) breathing is carried out based on the below stated Porstendorfer model[25].

$$DCF_M = 101\ x\ f_{Rn} + 6.7\ x\ (1 - f_{Rn} \quad (10)$$

$$DCF_N = 23\ x\ f_{Rn} + 6.2\ x\ (1 - f_{Rn}) \quad (11)$$

DCF for combined breathing (DCF_C)is evaluated using the relation below based on 60% from mouth and the rest of the nasal contribution to breathing[22,26].

$$DCF_C = 0.6\ DCF_M + 0.4\ DCF_N \quad (12)$$

The inhalation dose for mouth (ID_M) and nasal (ID_N) breathing is estimated by Eq. (13) based on the

human respiratory tract model stated by ICRP averaged over the lung[13,27].

$$ID = C_R \, x \, \frac{F_R}{3700} \, x \, \frac{7000h/y}{170} \, x \, DCF \quad (13)$$

2.3 Modeling Approach

Present study also predicts the pollutant behavior inside the domain using the computational fluid dynamic (CFD) method. The Fluidyn-VENTCLIM software based on the finite volume method was used to simulate ^{222}Rn and ^{220}Rn dispersion. Four different simulations were performed for studying ^{222}Rn and ^{220}Rn at open and closed room conditions. It solves mass and momentum conservation equations for indoor conditions and the details have been discussed elsewhere[16,28]. Geometry plotting is carried out using CAE-VENTCLIM and for simulation in build radon and thoron chains were used with different values of flux and boundary conditions. Initial gas concentration was assumed to be zero which grows according to the flow conditions. Gas concentration C (Bq/m^3) distribution in the domain is described as the relation below

$$\frac{\partial C}{\partial t} = S + \nabla.(D^*.C) - \nabla.(uC) - \lambda C \quad (14)$$

Where D^* (m^2/s) is the effective diffusion coefficient, source term (Bq m^{-3} s^{-1}) is represented by Sa nd λ account for the decay constant and u represents the velocity vector[29].

Radon and thoron exhalations from the different sources are their main source and considered that it is distributed uniformly over the contributing surfaces. A constant temperature was considered during the simulation. For simulating contaminant transport, the standard k-ε model was used with some constants as C_μ= 0.09, and the empirical dimensionless constants are σ_k=1.0, σ_ε=1.30, $C_{1\varepsilon}$=1.44, $C_{2\varepsilon}$=1.92. Boundary conditions are assumed to be non-slip at walls. Flow governing equations are discretised at every node and the distribution of any interesting variable can be found with the solutions of the corresponding algebraic equations.

3 Results and Discussion

This study elaborates the dispersion of ^{222}Rn,^{220}Rn and their decay products in a real room using measurement along with the computational modeling using CFD software. The study includes the affecting factors and necessary inputs for modeling.

Passive measurements for ^{222}Rn and ^{220}Rn concentration in the experimental room carried out using pin-hole dosimeters at three equidistant planes at different heights from the floor 0.8 m (P1), 1.6 m (P2), 2.4 m (P3). The time-integrated measurement and detector deployment are shown in Fig. 2.

In the experimental room, all the contributing surfaces exhale radon measured in terms of flux and the flux obtained are 0.41, 0.28 and 0.27 mBq m^{-2} s^{-1} from wall, floor and ceiling respectively. The experimental room walls are made of bricks and furnished with plaster, the roof is a concrete slab while the floor is covered with concrete mixture and marble chips. Source of thoron in the room is mainly from the room surfaces which exhales thoron 0.5 Bqm^{-2}s^{-1}. The measured flux values are comparable to the values proposed by Meisenberg *et al*., 2017 for walls covered by building material[23].^{222}Rn and ^{220}Rn concentrations in the room are measured using pinhole dosimeter and are depicted in Table 1, for ^{222}Rn and Table 2 for ^{220}Rn with position coordinates of measurement sites. Five measurement points are chosen such that one is the central point and four corners (C1, C2, C3, C4) of the room at 30 cm from the wall for the P2 plane while for the plane P1 and P3 passive measurements are carried out for the central point. Analysis of data shows higher radon levels for the closed room condition for all measurement points. In contrast to radon, the thoron levels do not show a significant and decorous behavior. The radon dispersion shows a more uniform behavior as compared to thoron.

The measurements of ^{222}Rn and ^{220}Rn concentrations are also executed using active measurement with SRM and STM for the two planes (P1 and P2) with five locations per plane. The measurement results are

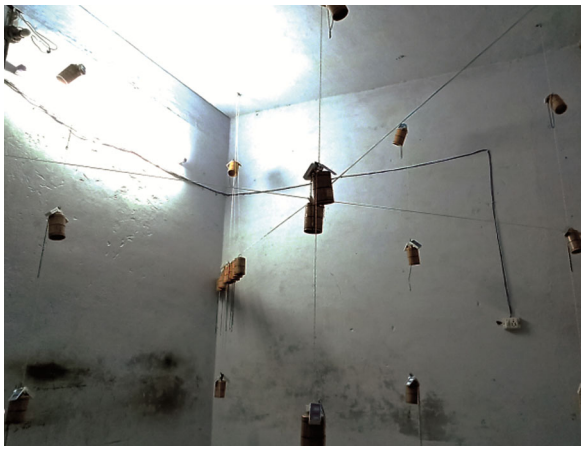

Fig. 2 — Deployment of dosimeters and progeny sensors in the room.

presented in Table 3 for radon and Table 4 for thoron. Higher concentration values are found for thoron as compared to radon. For the case of radon gas, the closed room condition is responsible for high radon level and during the open condition radon gas gets diluted with the external atmospheric air responsible for less concentration. Radon concentrations for the open condition are almost half of their values for the closed condition. Although all the measured concentrations are less than the recommended level[2]. Thoron shows irregular and unpredictable behavior, for the central point of both P1 and P2 planes thoron concentration is found higher for open as compared to closed room condition. This may be due to the reason that thoron being a short-lived gas that migrates a small distance in a comparatively calm environment while for the disturbed case thoron reach a high level at the center. Experimental measurement clears that the accumulation of gas is the consequence of the balance between the sources (exhalation from contributing surfaces) and removal processes (radioactive decay and ventilation mechanisms)[30]. For the open and closed room condition in the experimental room, simulation is also carried out using CFD software. Using the measured parameters; the case is setup in CFD software for the same experimental room. In order to investigate the ^{222}Rn and ^{220}Rn distribution and dispersion profiles using CFD model, the concentration dispersion contours are plotted and presented in Fig. 3. It shows the dispersion of ^{222}Rn and ^{220}Rn gas into the room environment from the source walls. Clearly and as expected ^{222}Rn and ^{220}Rn concentration is found more near the exhalating surface than in the rest of the room[9,31]. Effect of room ventilation condition can be clearly seen on the radon and thoron concentration level along with the dispersion pattern.

For the sake of comparison between all the study approaches and different room conditions, a graph is plotted, presented as Fig. 4 for radon and Fig. 5 for thoron. It compares the radon and thoron

Table 1 — Passive measurement results of radon concentration measured with dosimeters

Location	Co-ordinates	Open condition	Closed condition
		Radon concentration (Bq/m^3)	
Central point (Z= 0.8), CE-0.8	(1.5, 1.58, 0.8)	34.2 ± 10.1	56.4 ± 16.8
Corner 1 (Z= 1.6), C1-1.6	(0.3 2.86, 1.6)	26.2 ± 7.3	67.6 ± 11.3
Corner 2 (Z= 1.6), C2- 1.6	(2.7, 2.86, 1.6)	29.3 ± 11.2	50.9 ± 19.1
Corner 3 (Z= 1.6), C3- 1.6	(2.7, 0.3, 1.6)	30.5 ± 8.9	55.2 ± 18.0
Corner 4(Z= 1.6), C4- 1.6	(0.3, 0.3, 1.6)	24.9 ± 6.8	62.8 ± 16.4
Central point (Z= 1.6), CE-1.6	(1.5, 1.58, 1.6)	30.4 ± 8.7	54.8 ± 10.3
Central point (Z= 2.4), CE-2.4	(1.5, 1.58, 2.4)	31.3 ± 11.1	53.3 ± 15.1

Table 2 — Passive measurement results of thoron concentration measured with dosimeters

Location	Co-ordinates	Thoron concentration (Bq/m^3)	
		Open condition	Closed condition
CE-0.8	(1.5, 1.58, 0.8)	48.6 ± 10.4	31.3 ± 10.1
C1-1.6	(0.3 2.86, 1.6)	80.3 ± 12.5	75 .0± 19.0
C2- 1.6	(2.7, 2.86, 1.6)	45.6 ± 5.9	38.4 ± 11.2
C3- 1.6	(2.7, 0.3, 1.6)	82.5 ± 15.1	61.9 ± 16.0
C4- 1.6	(0.3, 0.3, 1.6)	59.8 ± 18.0	70.8 ± 17.3
CE-1.6	(1.5, 1.58, 1.6)	42.6 ± 9.2	25.7 ± 6.9
CE-2.4	(1.5, 1.58, 2.4)	45.3 ± 11.7	41.7 ± 9.9

Table 3 — Active measurement results of radon concentration measured with SRM

Radon level for XY plane at Z = 0.8 m (Bq/m^3)			Radon level for XY plane at Z = 1.6 m (Bq/m^3)		
Co-ordinates	Open condition	Closed condition	Co-ordinates	Open condition	Closed condition
(0.3 2.86, 0.8),C1-0.8	36.4 ± 8.1	66.1 ± 11.0	(0.3 2.86, 1.6) C1-1.6	29.3 ± 4.0	56.1 ± 11.2
(2.7, 2.86, 0.8), C2-0.8	26.3 ± 6.3	51.2 ± 7.3	(2.7, 2.86, 1.6), C2-1.6	30.5 ± 6.1	44.4 ± 10.1
(2.7, 0.3, 0.8), C3-0.8	32.8 ± 4.0	54.3 ± 8.2	(2.7, 0.3, 1.6), C3-1.6	24.9 ± 7.0	50.2 ± 8.0
(0.3, 0.3, 0.8), C4-0.8	25.5± 7.4	50.4 ± 6.6	(0.3, 0.3, 1.6), C4-1.6	26.7± 2.8	48.9 ± 6.9
(1.5, 1.58, 0.8), CE-0.8	25.2 ± 2.8	49.8 ± 5.7	(1.5, 1.58, 1.6), CE-1.6	28.2 ± 4.5	50.7 ± 8.5

Table 4 — Active measurement results of thoron concentration measured with STM

Thoron level For XY plane at Z = 0.8 m (Bq/m^3)			Thoron level For XY plane at Z = 1.6 m (Bq/m^3)		
Location	Open condition	Closed condition	Location	Open condition	Closedcondition
C1-0.8	62.7 ± 8.1	82 ± 9.9	C1-1.6	79.4 ± 9.1	78.3 ± 9.1
C2-0.8	51.6 ± 6.3	32 ± 5.6	C2-1.6	53.4 ± 9.0	28.1 ± 4.3
C3-0.8	63.8 ± 9.2	57 ± 5.8	C3-1.6	65.8 ± 8.9	61.8 ± 8.2
C4-0.8	43.6 ± 6.8	52 ± 8.2	C4-1.6	50.9 ± 6.6	41.4 ± 3.1
CE-0.8	51.3 ± 6.6	26 ± 5.7	CE-1.6	45.9 ± 8.5	21.3 ± 7.7

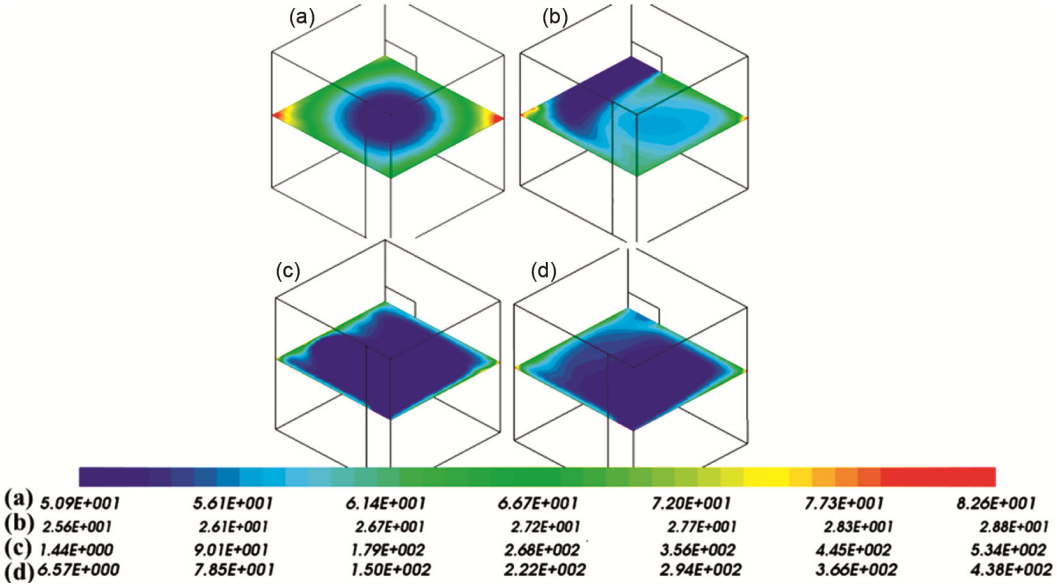

Fig. 3 — The contour of radon and thoron concentration at different room conditions using CFD simulation i. for radon at (a) close and (b) open condition ii. For thoron at (c) close and (d) open condition.

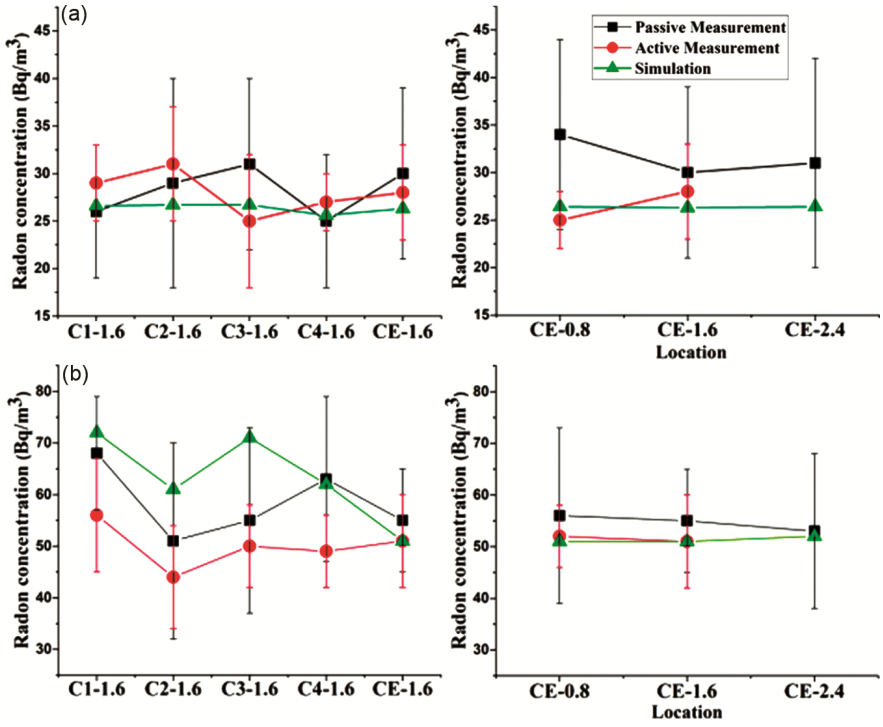

Fig. 4 — Comparison of simulation and experimental radon concentration measurements results (a) open (b) closed condition.

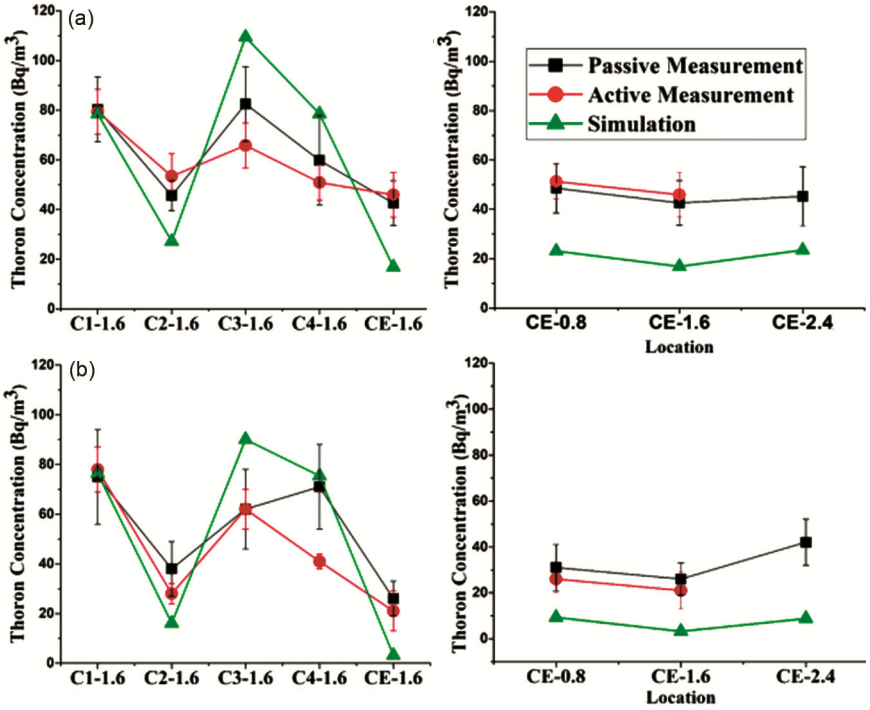

Fig. 5 — Comparison for thoron concentration estimated using simulation and experiment for (a) open and (b) closed condition.

concentration obtained from CFD modeling and experimental (passive and active) measurements along with their standard deviations. The comparison shows that the simulation and experimental (active and passive) measurements are close to each other. The estimated values are within the measurement range as presented in Fig. 4 & 5. The observed radon concentrations are found less than the reference level[32] and the concentration values are more than the worldwide average value of 37 Bq/m^3 for closed condition and similar for the open room condition[1,13]. Radon concentration is found more uniformly distributed for the open room condition (Fig. 4) while thoron show irregular and complex behavior. A decrease in radon level is found through prediction and measurement for open room condition with an increase of homogeneity as compared to non-mixing condition. Thoron level varies depending on the dosimeter and measurement location. This suggests the deployment of at least a few dosimeters for thoron measurement and exact dispersion pattern. The thoron level within the study room at different measuring positions might vary by their attributing distance, because of variable indoor air mixing for different condition. This result is in agreement with the study performed by Meisenberg *at al*., 2017 for dwelling with earthen and covered architecture[23].

Along with the dosimeters, progeny sensors are also deployed to measure equilibrium equivalent progeny concentration at all the desired locations. Measured equilibrium equivalent concentration values are depicted in Table 5 at different room condition for radon and thoron. Fig. 6 and 7 presents the variation of total EEC_{A+U} and unattached EEC (EEC_U) for radon and thoron respectively at open and closed room condition. For the case of radon total EERC and $EERC_U$ are found more for closed room condition as in the closed room there is less dilution with atmosphere which responsible for more total and unattached progeny level. Radon level are also higher for closed room condition (Table 1). For the case of

Table 5 — Passive measurement result of radon and thoron progeny concentration measured with DTPS and DRPS

EEC (Bq/m^3) at different condition	Minimum	Maximum	Average
Total EERC-Open	10.2	15.4	12.5 ± 0.7
Total EERC-Closed	17.8	21.7	19.1 ± 0.6
Total EETC-Open	1.4	2.6	1.9 ± 0.2
Total EETC-Closed	0.9	2.4	1.6 ± 0.2
EERC (A)-Open	8.8	13.7	11.4 ± 0.6
EERC(A)-Closed	13.8	17.9	15.5 ± 0.6
EETC(A)-Open	1.2	2.4	1.7 ± 0.2
EETC(A)-Closed	0.6	1.8	1.2 ± 0.2
EERC(U)-Open	0.8	1.4	1.1 ± 0.1
EERC(U)-Closed	3.0	4.1	3.4 ± 0.1
EETC(U)-Open	0.1	0.3	0.2 ± 0.0
EETC(U)-Closed	0.1	0.7	0.4 ± 0.2

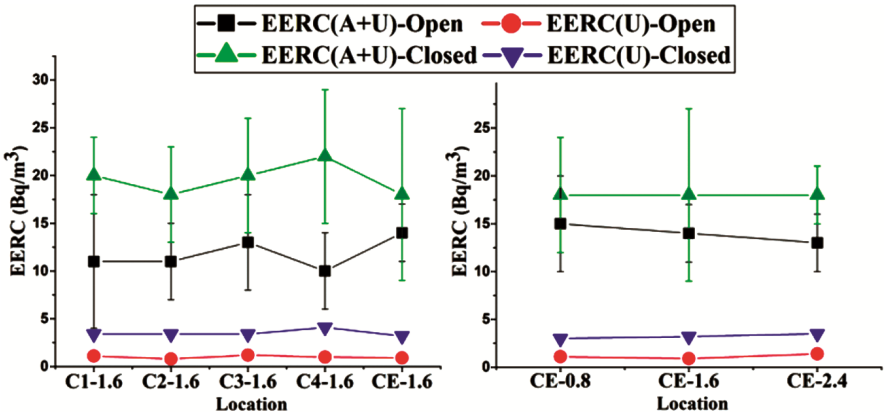

Fig. 6 — Variation of EERC for open and closed room condition.

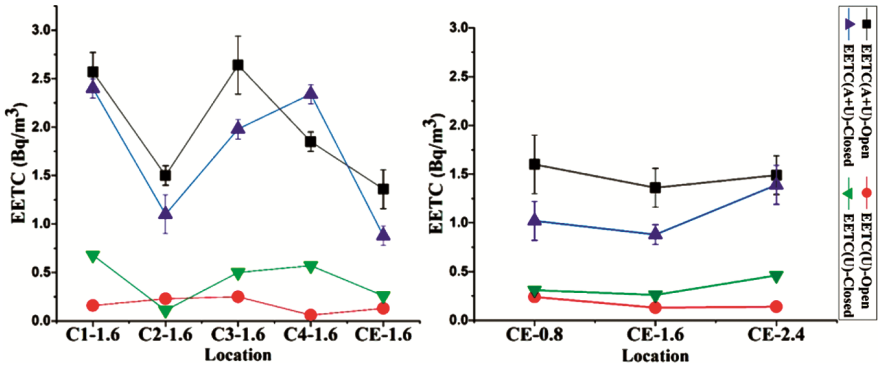

Fig. 7 — Variation of EETC for open and closed room condition.

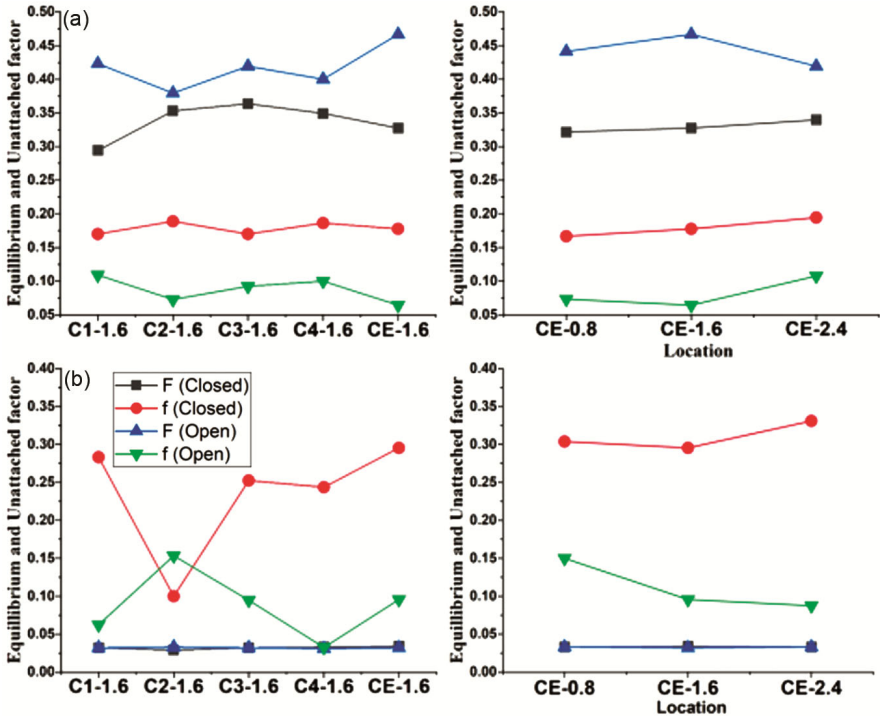

Fig. 8 — Equilibrium and unattached fraction variation and comparison (a) Radon (b) Thoron.

Table 6 — Calculated equilibrium factor, unattached fraction, estimated doses and conversion factors.

	Open condition			Closed condition		
	Min.	Max	Average	Min	Max	Average
Equilibrium factor (F_{Rn})	0.4	0.5	0.4 ± 0.01	0.3	0.4	0.3 ± 0.1
Unattached fraction (f_{Rn})	0.1	0.1	0.1 ± 0.01	0.17	0.2	0.2 ± 0.0
Equilibrium factor (F_T)	0.03	0.03	0.03 ± 0.0	0.03	0.03	0.03 ± 0.0
Unattached fraction (f_T)	0.03	0.2	0.1 ± 0.02	0.1	0.3	0.3 ± 0.03
DCF-mouth (mSv/WLM)	12.8	16.9	15.0 ± 0.7	22.4	25.0	23.6 ± 0.4
DCF-Nasal (mSv/WLM)	7.3	8.0	7.7 ± 0.1	9.0	9.5	9.2 ± 0.1
DCF-combined (mSv/WLM)	10.6	13.4	12.1 ± 0.4	17.0	18.8	17.8 ± 0.3
Inhalation Dose-mouth (ID_M) (mSv/y)	1.7	2.4	2.1 ± 0.1	4.5	5.9	5.0 ± 0.2
Inhalation Dose-Nasal (ID_N) (mSv/y)	0.9	1.2	2.1 ± 0.1	1.8	2.3	2.0 ± 0.1
Annual effective dose radon (AEDR)(mSv/y)	0.7	1.0	0.8 ± 0.04	1.2	1.5	1.3 ± 0.04
Annual effective dose thoron(AEDT)(mSv/y)	0.4	0.8	0.6 ± 0.1	0.3	0.7	0.5 ± 0.1
Total Annual effective dose (AED)(mSv/y)	1.2	1.7	1.4 ± 0.1	1.5	2.2	1.8 ± 0.1

thoron $EETC_{A+U}$ found more for open room while $EETC_U$ found more for closed room condition. As the thoron disperse more in disturbed open environment which is responsible for more EEC_{A+U} but the open environment is also responsible for more cluster formation that may give more $EETC_A$ hence less $EETC_U$, therefore in the closed environment unattached progenies are more as compared to attached[33]. Much variation is not found in the EERC values shows how the solid progenies distributes uniformly in the closed room. Unattached fraction and equilibrium factors are also calculated and presented in Fig. 8. Unattached and equilibrium factor are almost uniform for radon case at open and closed room condition while for thoron unattached fraction shows more variability and equilibrium factor is found uniform. Much variation in equilibrium is not found here for both radon and thoron, also the values are within the range of globally defined values for both ^{222}Rn and ^{220}Rn. The results for unattached and equilibrium factor are presented in Table 6. It is noted that the decay product concentration cannot be greater than that of its progenitor[13] therefore the F (^{222}Rn and ^{220}Rn) values cannot be >1. For lung dose assessments worldwide f values are 0.1 for ^{222}Rn, the calculated values in the present study for open room condition are in close agreement[34].

DCF associate radon and progeny exposure of an individual to the effective dose and is estimated individually for nasal and mouth breathing based on Porstendorfer model[25]. The DCFs are estimated for mouth, nasal and combined breathing using the relation (10, 11 and 12) and the calculated values are depicted in Table 6. Inhalation doses also estimated using the mouth and nasal DCFs. The inhalation dose found due to mouth breathing (ID_M) is 2.1± 0.1mSv/y for open and 5.0± 0.2mSv/y for closed room condition. A comparison of inhalation dose for different room condition is presented in Fig. 9. Table 6 represents the

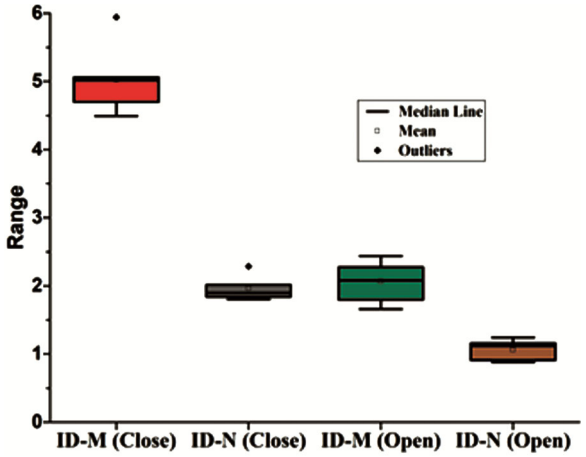

Fig. 9 — Inhalation dose for mouth (ID_M) and nasal (ID_N) breathing.

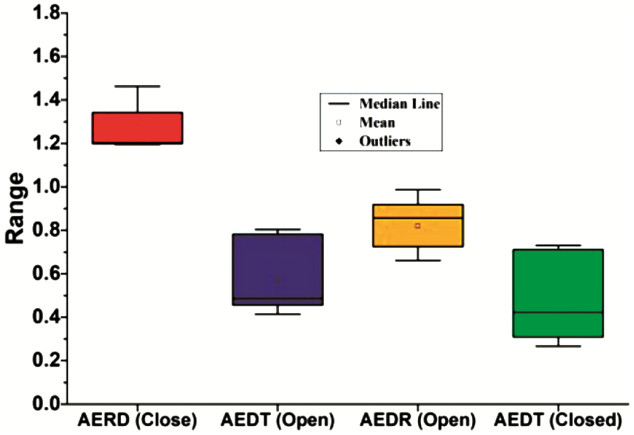

Fig. 10 — Annual effective dose for ^{222}Rn and $^{220}Rnat$ open and closed condition.

calculated factors and estimated doses for the present study. Concerning health impact on the residents in radioactive indoor, the quantity to be compared is considered as the inhalation dose. Health risk assessment due to exposure to ^{222}Rn and progeny exposure usually investigated by measurements of the ^{222}Rn concentration and the equilibrium factor[23,34]. The applicability of same for thoron is not considered because of its non-uniform behaviour, variability of F and unattached fraction[23,34]. Variation of annual effective dose is presented in terms of box plots in Fig. 10 for radon and thoron and Fig. 11 presents the box plot presentation of total effective dose received annually due to presence of ^{222}Rn, ^{220}Rn and decay products. The more contributor of the inhalation dose received are the progeny from both, ^{222}Rn and ^{220}Rn chains[23]. The analyzed results in annual dose contribution of 1.4 ± 0.1 mSv for open and 1.8 ± 0.1mSv for closed room condition from radon and thoron. The values of estimated effective dose received annually are within the reference range stated by ICRP from 3 to 10 mSv/y and also found below the (10 mSv/y) reference level[2,13,32].

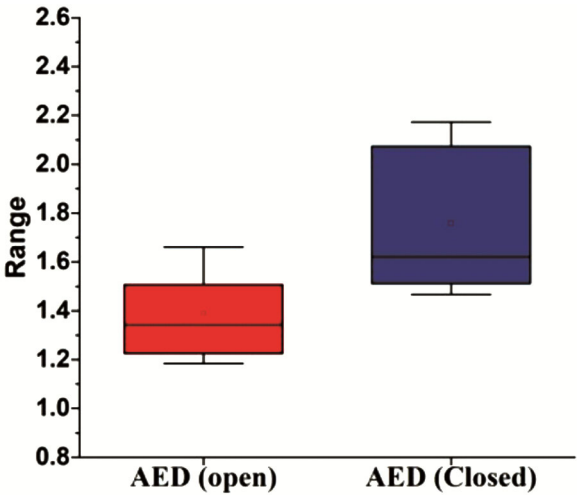

Fig. 11 — Total effective dose received annually for different room condition.

The distribution of ^{222}Rn and ^{220}Rn within the model domain can also be studies by height profiles from floor to ceiling varying from z = 0.2 m to z = 2.8 m in steps of 0.2 m. Profiles (Fig. 12) show the variability at four corners (C1 to C4) and room center (CE). At the corners the levels are high because the

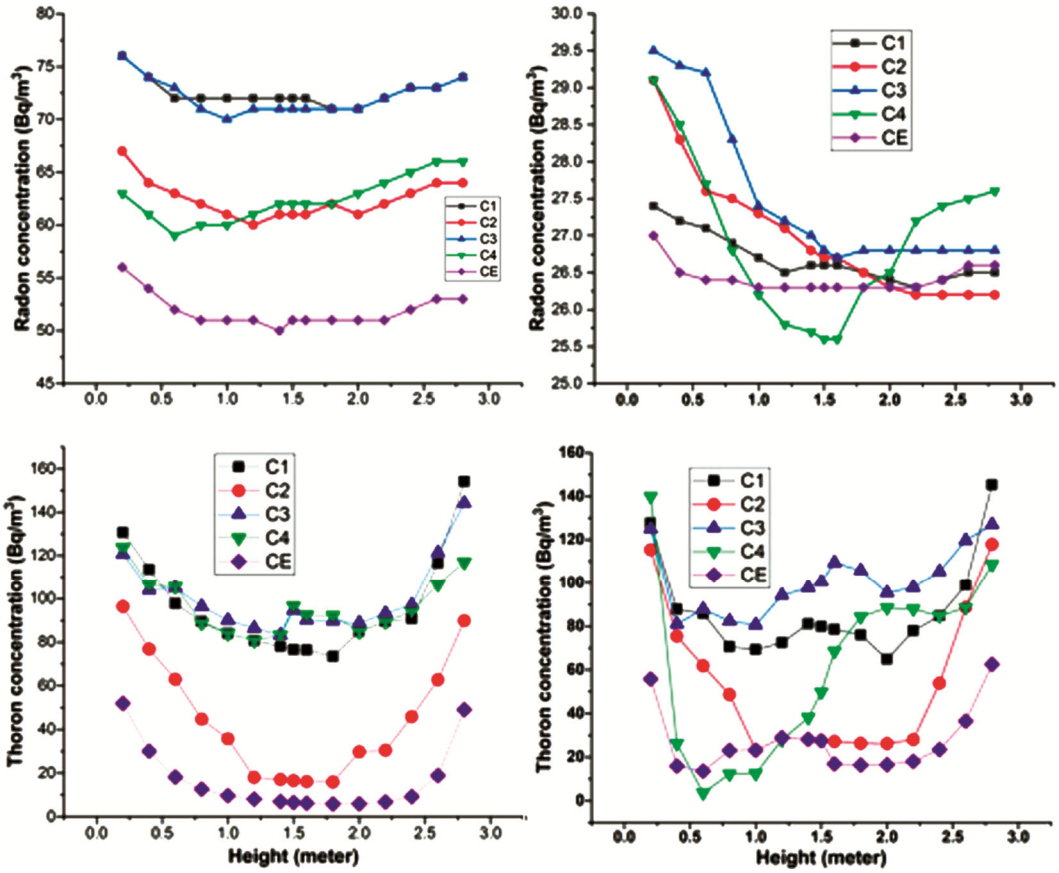

Fig. 12 — Height profile for radon and thoron concentration (a) radon inclose (b) radon inopen (c)thoron in close (d) thoronin open room.

contributing sources (walls) present close to them. Also, radon concentrations are almost uniform with height for the closed room condition while comparatively non uniformity is observed in open room condition. For the case of thoron uniformity is observed with height except the corners C2 and C4. This may be due to the presence of air diffusers here for open room condition. Different room environment is responsible for different pattern in terms of uniformity and non-uniformity especially for thoron.

Measurement of input parameters and study of ^{222}Rn, ^{220}Rn and progeny dispersion in the real experimental room are the highlights of this work. Agreement of modeling with experimental results makes it capable of predicting the radon and thoron behavior being less time consuming, cost effective and versatile, and distribution pattern for different conditions.

4 Conclusions

This study refers to a planned examination for radon-thoron and progeny in an indoor environment for the open and closed room condition. For the open room, the average $C_{Rn}(Bq/m^3)$ is found to be 29.5 ± 1.2 while 57.3 ± 2.2 for closed. For the open room, the average $C_T(Bq/m^3)$ is found to be 57.8 ± 6.4 while 49.3 ± 7.5 for closed condition. Radon levels are found to be uniform and higher for the closed condition while thoron shows non-uniform and complex behavior and the accumulation of gas is found to be in control of the sources and removal processes. The average $EERC_U$ (Bq/m^3) is found to be 1.1 ± 0.1 for open and 3.4 ± 0.1 for closed room. The average $EETC_U$ is found to be 0.2 ± 0.0 for open and 0.4 ± 0.1 for closed condition. $EERC_U$ and $EERC_{A+U}$ are found more for the closed room while $EETC_{A+U}$ is more for open and $EETC_U$ found more for closed environment. F_{Rn}, F_T and f_{Rn} are found uniform in the room for all study cases but f_T is distributed in-homogeneously. Different room environment is responsible for different pattern and level, especially for thoron. The diagonal profile for closed room shows the uniformity for radon while thoron decays rapidly with distance initially. Different dose conversion factors and inhalation and effective doses are also estimated and found within the recommended limits.

Acknowledgment

The authors are thankful to the Director and Head of the Department of Physics, NIT Kurukshetra, India, for providing experimental facilities.

References

1 UNSCEAR, 2000.Report to the General Assembly, with Scientific Annex B.
2 WHO, Indoor radon a public health perspective, A public health perspective, *Int J Environ Stud,* 2009.
3 Nazarof WW, Moed B A & Sextro RG, In: Radon and its decay products in indoor, 1988.
4 Yanchao S, Bing S, Hongxing C &Yunyun W, *Appl Radiat Isot*, 173 (2021) 109706.
5 Tokonami S, *Radiation Protection Dosimetry*, 141 (2010) 335.
6 Janik M, Tokonami S, Kranrod C, Sorimachi A, Ishikawa T, Hosoda M, Mclaughlin J, Chang BU & Kim YJ, *J Radiat Res*, 54 (2013) 597.
7 Nazir S, Simnani S, Mishra R, Sharma T & Masood S, J *Radioanal Nucl Chem,* 325 (2020) 315.
8 Takahashi L C, de Oliveira Santos T, Pinheiro R M M, Passos R G & Rocha Z, *Appl Radiat Isot*, 186 (2022) 110217.
9 Urosevic V, Nikezic D & Vulovic S, *J Environ Radioact*, 99 (2008) 1829.
10 Akbari K, Mahmoudi J & Ghanbari M, *J Environ Radioact*, 116 (2013) 166.
11 Chen J, Rahman N M & Atiya I A, *J Environ Radioact*, 101 (2010) 317.
12 Ramachandran T V, Eappen K P, Nair R N, Shaikh A N, Mayya Y S & PuranikV D, In Proceedings of the thirteenth national symposium on environment. Focal theme: mining of energy resources-environmental management, (2004).
13 Singh P, Saini K, Mishra R, Sahoo B K & Bajwa B S, *Radiat Environ Biophys*, 55 (2016) 401.
14 Gaware J J, Sahoo B K, Sapra B K & Mayya Y S, *Barc Newsl*, (2011) 45.
15 Devi V, Kumar A & Chauhan R P, *Environ Earth Sci*, 78 (2019) 506.
16 Chauhan N, Chauhan R P, Joshi M, Agarwal T K, Aggarwal P & Sahoo B K, *J Environ Radioact*, 136 (2014) 105.
17 Sahoo B K, Sapra B K, Kanse S D, Gaware J J & Mayya Y S, *Radiat Meas* 58 (2013) 52.
18 Mishra R, Sapra B K & Mayya Y S, *Nucl Instruments Methods Phys Res Sect B Beam Interact with Mater Atoms*, 267 (2009) 3574.
19 Mayya Y S, Mishra R, Prajith R, Sapra B K & Kushwaha H S, *Sci Total Environ*, 409 (2010) 378.
20 Mishra R & Mayya Y S, *Radiat Meas*, 43 (2008) 1408.
21 Knutson EO, In: Nazaroff WW, Nero AV JrRadon and its decay products in indoor air, Wiley, NewYork, (1988) 161.
22 Mehra R, Jakhu R, Bangotra P & Mittal H M, *Dose-Response*, 14 (2016) 1.
23 Meisenberg O, Mishra R, Joshi M, Gierl S, Rout R, Guo L, Agarwal T, Kanse S, Irlinger J, Sapra B K & Tschiersch J, *Sci Total Environ*, 579 (2017) 1855.
24 UNSCEAR, Sources and effects of ionizing radiation. United Nations, New York, Report to the General Assembly, with Scientific Annexes, 2008.
25 Porstendörfer J, *Environ Int*, 22 (1997).
26 Bennett W D, Zeman K L & Jarabek A M, *J Toxicol Environ Heal - Part A Curr*, 71 (2008) 227.
27 ICRP, ICRP Publication-65, Protection against radon-222 at home and at work, Pergamon Press, Oxford, 1993.

28 Devi V & Chauhan R P, *Radiat Environ Biophys*, 60 (2021) 309.

29 Agarwal T K, Sahoo B K, Gaware J J, Joshi M & Sapra B K, *J Environ Radioact*, 136 (2014) 16.

30 Xie D, Wu Y, Wang C, Yu CW, Tian L & Wang H, *Sustain Cities Soc*, 66 (2021) 102599.

31 Zhou W, Iida T, Moriizumi J, Aoyagi T & Takahashi I, *Radiat Prot Dosimetry*, 93 (2001) 357.

32 ICRP, ICRP publication 115: lung cancer risk from radon and progeny and statement on radon, Ann ICRP, Pergamon Press, Oxford, (2011).

33 Porstendorfer J, Tutorial / review properties and behaviour of radon and thoron and their decay products in the air, 25 (1994) 219.

34 UNSCEAR, Annex E: sources-to-effects assessment for radon in home and workplaces. United Nations, New York Report to the General Assembly, (2006).